Materials Science and Engineering B 121 (2005) 238–243

MATERIALS SCIENCE & ENGINEERING B

www.elsevier.com/locate/mseb

Studies on the surface swelling of ion-irradiated silicon: Role of defects

P.K. Giri *

Department of Physics, Indian Institute of Technology Guwahati, North Guwahati 781039, India

Received 25 November 2004; received in revised form 6 April 2005; accepted 8 April 2005

Abstract

Low-energy (keV) Si ions are implanted on mask-pattered Si wafer at doses above amorphization threshold for a variety of implantation conditions (ion dose, energy, temperature) and post-implantation annealing. Precise measurement of the surface swelling (step-height) on the amorphous Si layer was carried out using an atomic force microscope (AFM). Thickness and microstructure of the ion-damaged layer was evaluated by transmission electron microscopy (TEM) measurements. The measured step-height in excess to that contributed by implanted ions shows a cube root dependence on the Si ion dose. The swelling heights studied for two different energies of Si ions show identical step-heights. Implantation at low temperature (77 K) shows a reduced step-height, indicating possible contribution of migrated Si atoms in the swelling. We propose that excess swelling is caused by migration and segregation of the displaced Si atoms from the bulk to the surface leaving behind corresponding vacancies in the lattice. Ellipsometric studies of the similarly damaged layer profile provide supporting evidence for surface segregation of Si atoms over the amorphous layer.

Keywords: Ion implantation; Surface swelling; Silicon; Electron microscopy; Atomic force microscopy

1. Introduction

Ion implantation is widely used for doping and various other applications in semiconductor device fabrication. During high dose implantation the accumulated damage due to lattice displacements gives rise to amorphous structure, which may depend on various parameters of implantation. In the literature, ion implantation-induced amorphization has been associated with a change in volume or density of the host material, which results in surface expansion or swelling (a change in linear dimensions) of the implanted region [1,2]. Experiments with materials to be used as a first wall for future reactors have revealed that relative elongation of β-SiC under neutron irradiation can be as high as 0.7% [3]. The swelling effect has been observed in a variety of other common semiconductors such as Si, Ge, SiC, GaAs, etc. However, the exact mechanism behind such expansion in Si has not been understood properly. Studies on amorphized regions of Ge [4] and GaSb [5] have shown that formation of nanopores or voids is responsible for the swelling of the implanted region. However, no such nanostructures have been found in ion-implanted amorphous Si. There has been some indication about uniaxial lattice expansion in ion-implanted Si [6], but its magnitude was found substantially larger than the predicted value in uniaxially strained crystalline silicon, indicating possible contribution from other sources. Swelling effect has been observed in diamond and has been explained assuming that the amorphous region contains vacancy-rich regions [7]. Similarly, He-implanted Si has shown surface swelling [8]. Tamulevicius et al. [9] proposed a simple model for radiation swelling in silicon. However, detailed quantitative studies have not been performed on the mechanism of swelling in silicon. Positron annihilation studies on silicon indicate that vacancy clusters are formed in the ion-damaged region [10–12]. On the basis of swelling studies, ion-implanted pure amorphous Si (a-Si) was believed to be 1.7% less dense that crystalline Si (c-Si) [1]. However, contribution from point defects to density change has not been taken into account.

* Tel.: +91 3612582703; fax: +91 3612690762.
E-mail address: giri@iitg.ernet.in.

0921-5107/$ – see front matter © 2005 Elsevier B.V. All rights reserved.
doi:10.1016/j.mseb.2005.04.003

In this work, we have studied the swelling effect in ion-implanted Si for a wide range of ion dose, ion-energy, implantation temperature and post-implantation annealing conditions. Swelling height is precisely measured using atomic force microscopy (AFM), while thickness and microstructure of the amorphous layer were measured by cross-sectional transmission electron microscopy (XTEM). We argue that surface-migrated Si atoms primarily contribute to the extra physical step-height in the implanted region.

2. Experimental details

CZ grown Si (1 0 0) wafers were used for the present study. Using photoresist mask of varying stripe width (0.2–5.0 μm) on Si wafer, alternating stripes of amorphous Si (a-Si) and crystalline Si (c-Si) were produced by 80 keV Si ions implanted at room temperature to various doses in the range 6×10^{14} to 6×10^{16} ions/cm^2. After removal of the photoresist mask, the step-height (swelling) at the boundary between implanted and unimplanted region was measured using an AFM. Measured heights at several stripes were averaged for sufficient accuracy in swelling data. The horizontal scan length for the AFM measurement was chosen to cover about five alternating stripes of implanted and unimplanted regions, which allows averaging of the measured swelling. The thickness and quality of the amorphous layer was measured with XTEM. Post-implantation isochronal annealing was carried out at various temperatures in the range 450–1200 °C in steps of 200 °C in flowing N_2 gas and swelling was measured after each step of annealing.

3. Results and discussions

Fig. 1 shows a typical AFM image of the 80 keV Si implanted on the masked Si wafer at a dose of 6×10^{15} ions/cm^2 subsequent to the removal of the photoresist mask. Sharp vertical steps between implanted and unimplanted regions due to surface swelling in the ion-damaged layer are clearly seen in the figure. Typically several nanometers of step-heights are observed depending on the ion dose. The spike-like structure seen at the edge of the implanted region results from the residual photoresist layer at the boundary. The actual swelling is measured by using the flat portion of the image and averaging it over multiple stripes. It is found that difference in measured values for several stripes show variation much below 0.5 nm. Due to atomic resolution in the scanning probe, AFM technique offers quite high resolution compared to other conventional methods of step-height measurements.

Fig. 2 shows a plot of measured step-height for three different doses of Si implants as a function of stripe width. At lower doses, swelling is found to be independent of the stripe size, whereas at higher dose (i.e., 6×10^{16} ions/cm^2) it shows clear stripe size dependence. In particular, for stripes below 3.0 μm step-height reduces with lowering stripe widths. Similar observation has been made for 80 keV He-implanted silicon at a dose of 6×10^{16} ions/cm^2 [8]. However, saturated step-height with He implants was comparatively less than the height measured for Si implants, primarily due to the difference in ion mass. Note that the minimum dose used in this work corresponds to amorphization dose for Si, and with increasing dose the thickness of the amorphous layer increases and becomes uniform. During the amorphization of the implanted Si layer, defect interaction takes place. At shorter stripe width, migrating defects in the adjacent layer may interact and due to the annihilation of defects, swelling height is reduced. Further, in the implanted layer vertical strain is higher than the horizontal strain in the layer. In case of closely

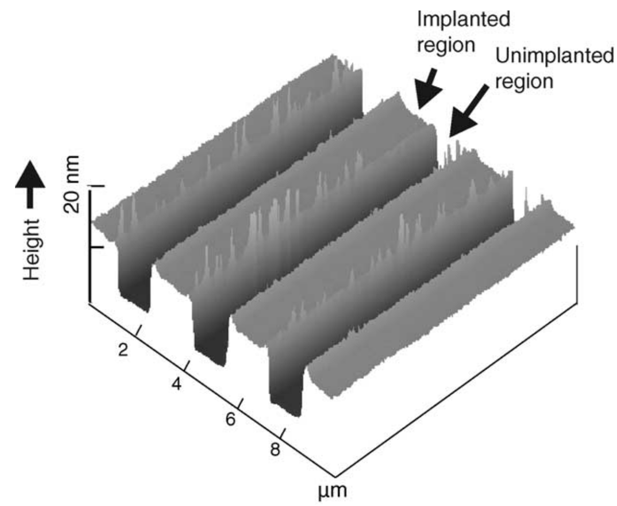

Fig. 1. An AFM image of the step-height (swelling) observed in 80 keV Si^+-implanted at room temperature on a masked Si wafer, with dose 6×10^{15} ions/cm^2. Unimplanted region corresponds to masked region of implantation.

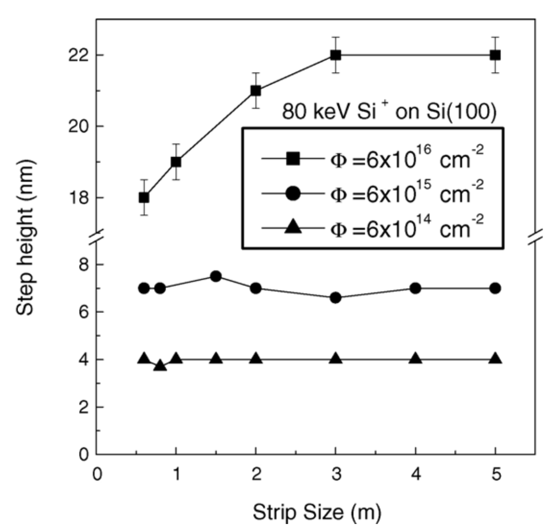

Fig. 2. Step-height plotted as a function of stripe-width of masked Si wafers for three different doses: 6×10^{14}, 6×10^{15} and 6×10^{16} ions/cm^2. At higher doses, clear stripe size dependence of swelling is observed below 3.0 μm stripe size. Dotted line passing through the data points is a guide to the eye.

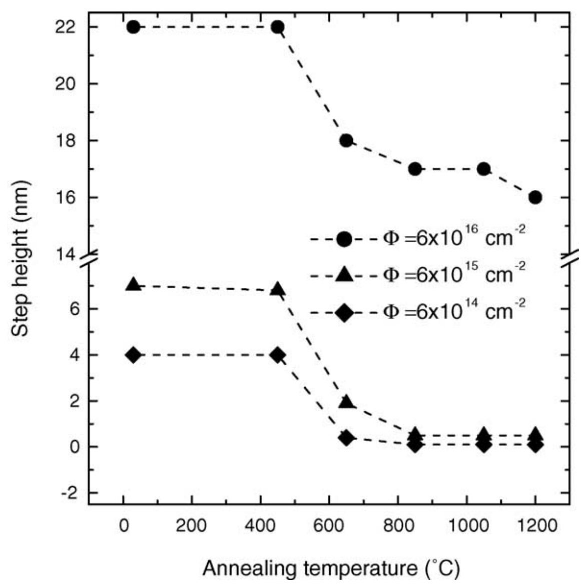

Fig. 3. Measured step-height after annealing at various temperatures for three different doses.

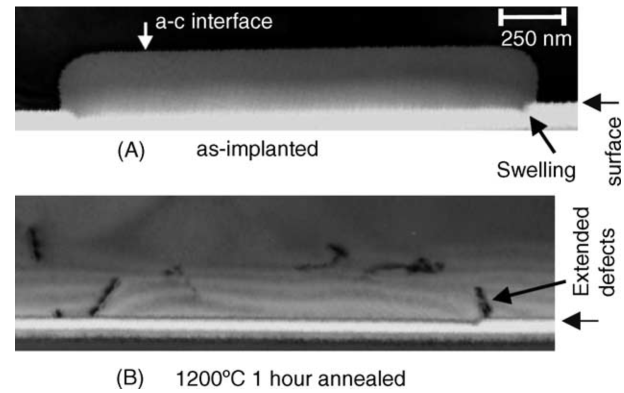

Fig. 4. Dark field XTEM image of the 80 keV, 6×10^{15} ions/cm^2 Si-implanted Si: (A) as-implanted and (B) 1200 °C annealed. Extended defect formation due to annealing is shown with arrow. Thickness of the amorphous layer is measured from the XTEM image.

spaced stripes, interaction of the induced strain from adjacent stripes in the damaged layer may cause relaxation of strain resulting in lesser step-height. The effect is pronounced when implanted ions themselves add measurable volume in the host lattice as in the case of very high dose and heavy ion implants. We have used the saturation value of step-height in each case for quantitative analysis.

In Fig. 3, the annealing characteristic of the swelling is shown as a function of step-by-annealing temperatures for three different doses. For different doses, the swelling decay characteristic as a function of temperature is found to be similar. Annealing at 450 °C does not show any measurable change in the step-height. However, a marked reduction in swelling is observed upon annealing at 650 °C for all the samples, and the swelling reduces nearly exponentially with temperature upon further annealing up to 850 °C, indicating a thermally activated process. Finally, the step-height reduces to a minimum after annealing at 1200 °C, though lower dose samples recover at a relatively lower temperature as shown in Fig. 3. Note that for the highest dose (6×10^{16} ions/cm^2), the residual step-height of 16 nm after 1200 °C annealing is larger than the height contributed by the implanted ions, assuming their rearrangement on a perfect crystalline Si (1 0 0) lattice. The pure a-Si layer is known to regrow at or above 550 °C and we observe a change in height at 650 °C due to the recrystallization. However, if the excess step-height was contributed by the lattice expansion only the step-height would be negligible after recovery of the a-Si layer. Usually the defects present in the amorphous layer partially anneals out at a lower temperature. However, in case of high dose implantation the ion-damage related lattice strain is partly released by the formation of extended defects during annealing. Fig. 4 shows cross-sectional TEM images of the ion-implanted (at a dose of 6×10^{16} ions/cm^2) layers before and after annealing at 1200 °C. The as-implanted sample shows a uniform amorphous layer whose thickness varies with ion dose, and a sharp amorphous–crystalline (a/c) interface is seen for high dose. Upon annealing up to 1200 °C, extended defects such as dislocations are formed at the original a-Si/c-Si interface as shown in Fig. 4(B). Therefore, the extra step-height in the annealed sample can be related in part to the volume occupied by the extended defects in the a/c interface. During the high dose implantation, point defects that escape direct recombination form defect clusters due to their close proximity, and must contribute to the structure of the a-Si in the subnanometer length scale. These defect clusters show high thermal stability; in particular, the vacancy clusters in silicon can be stable up to as high as 800 °C depending upon the ion dose [13,14]. In pure a-Si, direct evidence for the dominance of pentavacancy and hexavacancy clusters have been obtained from positron lifetime studies [12]. In the present case, the annealing behavior shown in Fig. 2 also suggests that higher order vacancy clusters are present in pure a-Si.

To understand further the contribution of defects, we have studied the effect of ion-energy on the swelling height. Fig. 5 shows XTEM images of the a-Si layer that are formed with 80 and 40 keV Si ions at a dose of 6×10^{15} ions/cm^2. In both

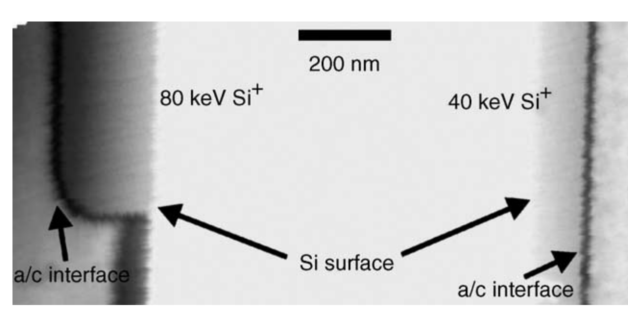

Fig. 5. XTEM image showing the comparison of a-Si layer thickness for 40 and 80 keV Si implants on Si at a dose 6×10^{15} ions/cm^2. Implant (40 keV) shows a thickness of about half that of the 80 keV implant, though swelling was identical in both cases.

cases uniform amorphous layer is formed from the surface. The thickness of the amorphous layer is found to be ∼210 nm for 80 keV and ∼110 nm for 40 keV Si ions. However, AFM measurements show exactly identical swelling in both cases. If the swelling has to occur due to lattice expansion in the amorphous layer, different layer thickness would give rise to different swelling height, which is contrary to our observation. Hence, lattice expansion proposed in the literature [6] cannot fully account for the observed swelling. Oxygen ion-implanted amorphous Si layer showed a swelling of 22 nm for amorphous layer-thickness of only 50 nm [15]. Therefore, swelling could not be related to the lattice expansion. These results have been explained on the basis of plastic flow of materials under irradiation [16]. Plastic flow of materials has been explained to be a result of spatial distribution of the vacancies and interstitial atoms [17]. In silicon, suppression of the radiation swelling at high temperatures of the substrate or high beam-current densities has been explained by the annihilation of radiation defects [12]. For such a defect-mediated process, the radiation swelling is expected to have a maximum at an elevated temperature. For low temperature it is limited by the slow diffusion process; when at high temperatures dynamic annealing and recrystallization of the implanted sample takes place.

We further studied the effect of implantation temperature on the swelling height. Implantation at low temperature (77 K) showed reduced swelling (20 nm) as compared to the swelling measured for room temperature (296 K) implants (22 nm) at a dose 6×10^{16} ions/cm^2. Since the implantation-induced point defects are less mobile at low temperature and a fraction of these defects do not reach the surface, the reduced swelling is clearly indicative of the defect-controlled mechanism for the growth of the excess swelling. However, at 77 K Si interstitials are quite mobile as compared to the Si vacancies. Therefore, reduction in swelling is not so substantial at 77 K. We believe that effect of implantation temperature on swelling would be more pronounced for implantation at cryogenic temperatures (<10 K).

Table 1 shows the measured swelling height and thickness of the a-Si layer for different doses. Measured swelling exhibits a sublinear dependence on the dose. The damage evolution leading to amorphization in Si is also known to vary sublinearly with dose due to dynamic annealing of defects.

Table 1
Summary of the measured data for a-Si thickness (*d*) and step-height (*h*) for various doses of Si implantation

Dose (ions/cm^2)	*d* (nm)	Measured *h* (nm)	Expected *h* due to ions volume (nm)	Excess *h* (nm)
6.0×10^{14}	128	4	0.12	3.92
1.6×10^{15}	196	6	0.32	5.80
6.0×10^{15}	209	7.5	1.21	6.76
1.8×10^{16}	232	12	3.63	9.79
3.6×10^{16}	236	17	7.26	12.59
6.0×10^{16}	248	22	12.10	14.65

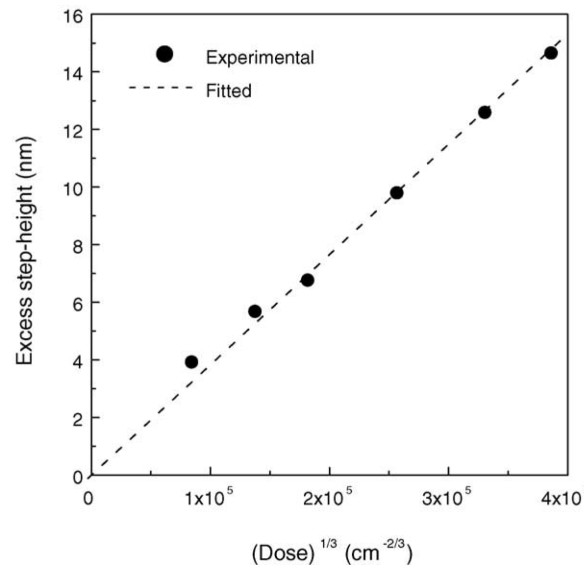

Fig. 6. Excess step-height as a function of cube root of dose in as-implanted Si. The dashed line represents a linear fit to the experimental data passing through the origin.

For a quantitative understanding, the extra height added by the implanted ions and sputtering effect must be taken into account. To calculate the height added by the implanted ions, it is assumed that extra atoms are arranged on the (1 0 0) planes of the original Si lattice and sputtering induced removal of the Si layer has been taken into account. Thus the calculated/expected step-height due to the volume occupied by the ions and excess step-height are shown in Table 1.

Dose dependence of the excess step-height is plotted in Fig. 6, where the experimental data are shown with symbols. Excess step-height shows a cube root dependence on dose as evidenced by the linear fit passing through the origin (dashed line). This is very similar to the cube root dose dependence of strain in ion-implanted Si reported by Tamulevicius et al. [9], and cube root dose dependence of the vacancy concentration in Si reported by Krause-Rehberg and Leipner [18]. In both cases, defect-mediated process was proposed for the observed effect. This striking similarity of the dose dependence for vacancy concentration and excess step-height in self-ion-implanted Si strongly suggest a correlation between vacancy concentration and swelling in ion-irradiated Si. The annealing behavior of the swelling shown in Fig. 3 is qualitatively similar to the annealing of open volume defects in heavily damaged silicon [18].

The annealing characteristics of the observed swelling strongly suggest that the region directly modified by the ions contains excess vacancies or open volume defects. Despite the incorporation of extra ions in the lattice during implantation, the presence of excess vacancies in the bulk would imply that a fraction of the displaced silicon atoms must migrate to the surface and should contribute to the swelling. In keV ion-implanted Si, the displaced atoms due to their close proximity to the surface can migrate toward the surface and leaves excess vacancies in the damaged region. The change in average bond length and the distortion in bond angle result in a structure with more open volume than that present in crystalline Si [19]. We also note that at high dose, with increasing dose the change in thickness of the amorphous layer is not as much as the change in step-height (see Table 1). Hence, swelling is primarily caused by the Si atoms that have migrated towards the surface. Our explanation is fully consistent with the observation made in Ref. [8] for He-implanted Si that showed a swelling of 10 nm as compared to the swelling of 22 nm measured for Si implants. For identical energy and dose, He, being a lighter atom than Si, creates less displacement damage in Si and correspondingly a fewer atoms migrate to the surface resulting in lesser swelling. Studies with He implantation showed that number of silicon atoms in the step-height was nearly equal to the number of vacancies in the bubbles formed inside the implanted Si [8] layer. Hence, surface migration of atoms occurs irrespective of the ion species.

More direct evidence for the accumulation of Si atoms at the surface comes from ellipsometric study of Ar-ion-damaged Si layer. For this purpose, 120 keV Ar-ions are implanted on Si (1 0 0) wafers above amorphization threshold doses and spectroscopic ellipsometry measurements were performed to model the a-Si layer with a rotating polarizer type ellipsometer in the photon energy range 1.8–5 eV. Imaginary part of the pseudodielectric function (ε_2) is plotted as a function of energy in Fig. 7 for two different doses. To obtain a proper fit to the experimental data, effective medium approximation was used to model the ion-damaged layers

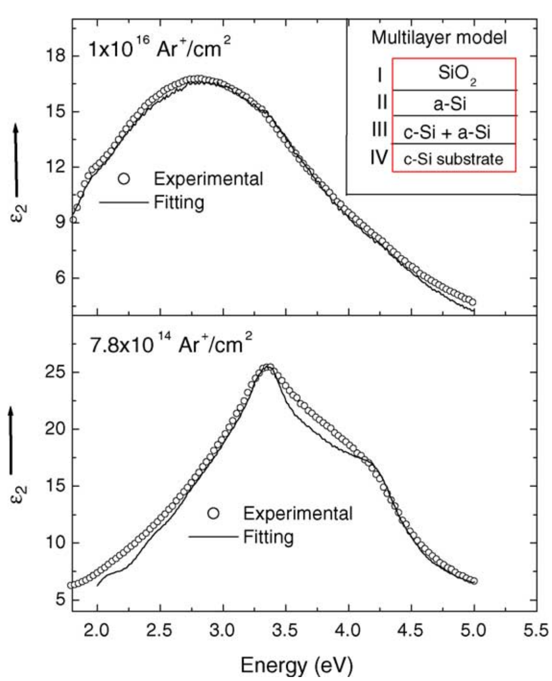

Fig. 7. Imaginary part of the pseudodielectric functions (ε_2) of Ar-implanted amorphus Si layer fitted with a multiplayer model to show the presence of a-Si (layer II) over the ion-damaged layer (layer III). Symbols show the experimental data, solid line shows the fitted data in each case. Inset shows the multilayer model used for the fitting using effective mass approximation.

consisting of the layers I–IV as shown in the inset of Fig. 7. The experimental data is shown with symbol (open circles) and the fitted data is shown as solid line in Fig. 7 for two different doses. More details of this fitting procedure can be found elsewhere [20]. Our analysis showed that besides the thick a-Si layer produced by the direct beam, there is a thin amorphous Si layer (thickness of a few nm) just above the original Si surface and beneath the native oxide layer in all implanted samples. This near-surface a-Si layer (layer II) thickness is about 5 nm and it is comparable to the oxide thickness (layer I) measured for different doses. Layer II merges with layer III for very high dose implantation, whereas at lower doses layers II and III can be distinctly identified with the help of fitting. At lower dose, layer III is a mixture of a- and c-Si fraction and with increasing dose c-Si fraction diminishes to zero. This layer II is believed to originate from the redistribution of migrated Si atoms produced by displaced atoms from the buried damaged region towards the surface and to a subsequent segregation process. Note that the amorphous layer thickness measured by ellipsometry in Ar-implanted Si is quite similar to the thickness measured in Si-implanted Si using TEM imaging. Therefore, ellipsometric results constitute a direct verification of the fact that Si atoms indeed migrate to the surface during the room temperature implantation and contribute to the swelling. Lohner et al. [21] have made similar observations in heavy-ion-implanted silicon. Our studies also show that at very high doses, contribution of the oxide layer (layer I) would be important for a more accurate analysis of the swelling in Si [20].

It may be noted that the surface expansion is likely to be different quantitatively for low-energy (keV) and high-energy (MeV) ion implantation due to the different depths of the defects created. At the keV energy range, lower energy ions would produce lesser displacements resulting in lesser step-height. However, as the lower energy ions produce displacement close to the surface, probability of interstitial Si atoms to migrate to the surface is more before recombining with the vacancy and hence more atoms would segregate on the surface, which compensates for the lesser displacements per atom finally resulting in same step-height. A closer look at the fitting of Fig. 6 reveals that for lower dose, step-height is higher than that expected from cube root dose dependence. With increasing dose, the a-Si layer thickness grows and displaced Si atoms is likely to get trapped by the already present damaged layer resulting in a lesser step-height than that expected from undamaged layer. Correspondingly, step-height at lower doses is found to be higher than that expected from cube root dose dependence. Hence, cube root dose dependence of step-height is more appropriate for high dose regime.

4. Conclusions

Surface swelling of self-ion-implanted silicon has been investigated as a function of ion dose, energy, implantation temperature and post-implant annealing conditions. Implantation temperature and energy dependence of the swelling clearly suggest the involvement of ion-induced defects in the measured swelling. Swelling height in excess to that contributed by implanted ion volume is argued to originate from the out-diffusion and segregation of the displaced Si atoms on the surface and thereby leaving corresponding number of excess vacancies in the host material. Spectroscopic ellipsometry studies provide supporting evidence for surface segregation of the displaced Si atoms.

Acknowledgements

We are thankful to Dr. V. Raineri for helps in various experiments. Fruitful discissions with Prof. E. Rimini is gratefully acknowledged.

References

[1] J.S. Custer, M.O. Thompson, D.C. Jacobson, J.M. Poate, S. Roorda, W.C. Sinke, F. Spaepen, Appl. Phys. Lett. 64 (1994) 437.
[2] W.G. Spitzer, G.K. Hubler, T.A. Kennedy, Nucl. Instrum. Meth. 209/210 (1983) 309.
[3] V.A. Borodin, A.E. Ryazanov, D.G. Sherstennikov, J. Nucl. Mater. 202 (1993) 169.
[4] H. Huber, W. Assmann, S.A. Karamian, A. Mucklich, W. Prusseit, E. Gazis, R. Grotzschel, M. Kokkoris, E. Kossionidis, H.D. Mieskes, R. Vlastou, Nucl. Instrum. Meth. B 122 (1997) 542.
[5] R. Callec, A. Poudoulec, J. Appl. Phys. 73 (1993) 4831.
[6] O.W. Holland, J.D. Budai, C.W. White, Appl. Phys. Lett. 57 (1990) 243.
[7] J.F. Prins, T.E. Derry, J.P.F. Sellschop, Phys. Rev. B 34 (1986) 8870.
[8] V. Raineri, S. Coffa, E. Szilagyi, J. Gyulai, E. Rimini, Phys. Rev. B 61 (2000) 937.
[9] S. Tamulevicius, I. Pozela, M. Andrulevicius, Mater. Sci. Eng. B 40 (1996) 141.
[10] S. Eichler, J. Gebauer, F. Broner, A. Polity, R. KrauseRehberg, E. Wendler, B. Weber, W. Wesch, B. Borner, Phys. Rev. B 56 (1997) 1393.
[11] A.P. Knights, G.R. Carlow, M. Zinke-Allmang, P.J. Simpson, Phys. Rev. B 54 (1996) 13955.
[12] G. Amarendra, R. Rajaraman, G. Venugopal Rao, K.G.M. Nair, B. Viswanathan, R. Suzuki, T. Ohdaira, T. Mikado, Phys. Rev. B 63 (2001) 224112.
[13] V.C. Venezia, D.J. Eaglesham, T.E. Haynes, A. Agarwal, D.C. Jacobson, H.-J. Gossmann, F.H. Baumann, Appl. Phys. Lett. 73 (1998) 2980.
[14] J. Xu, E.G. Roth, O.W. Holland, A.P. Mills Jr., R. Suzuki, Appl. Phys. Lett. 74 (1999) 997.
[15] K.N. Tu, P. Chenhari, K. Lal, B.L. Crowder, S.I. Tan, J. Appl. Phys. 43 (1972) 4262.
[16] C.A. Volkert, J. Appl. Phys. 70 (1991) 3521.
[17] Yu.V. Trushin, Tech. Phys. 39 (1994) 564.
[18] R. Krause-Rehberg, H.S. Leipner, Positron Annihilation in Semiconductors—Defect Studies, Springer-Verlag, Berlin, 1999 (Chapter 4).
[19] K.M. Beardmore, N. Gronbech-Jensen, Phys. Rev. B 60 (1999) 12610.
[20] P.K. Giri, S. Tripurasundari, G. Raghavan, B.K. Panigrahi, A.K. Tyagi, K.G.M. Nair, J. Appl. Phys. 90 (2001) 659.
[21] T. Lohner, M. Fried, N.Q. Khanh, P. Petrik, H. Wormeester, M.A. El-Sherbiny, Nucl. Instrum. Meth. Phys. Res. B 147 (1999) 90.